



Special Feature: Electronic and Optical Devices

Research Report

Light-induced Self-written Optical Waveguides

Manabu Kagami, Tatsuya Yamashita, Masatoshi Yonemura and Takayuki Matsui

Report received on Mar. 31, 2011

■ **ABSTRACT** ■ Light-induced self-written (LISW) technology is a unique and simple method of forming low-loss 3-dimensional (3-D) optical circuits in photopolymers using radiation from an optical fiber. Since this technology is applicable to almost all kinds of optical fiber and optical wiring, many studies have been carried in a number of different organizations on the applications of this technology. The technology helps simplify optical interconnections, and it is expected that it will reduce the cost of mounting optical devices. In this paper, we introduce LISW technology and report on related studies developed in our research group.

■ **KEYWORDS** ■ Light-induced self-written, LISW, Polymer optical waveguide, WDM, Photopolymer

1. Introduction

In large-scale systems, fiber-optic communications are already widely used. In recent years, though, optical fiber networks have been brought into the household, with applications such as consumer electronics, FTTH (Fiber to the home), and automotive applications. For these applications, low cost, low weight systems with a minimal number of cables are very much desired in order to facilitate installation. In order to achieve high-speed data transmission at low-cost with a minimum number of cables, WDM optical communication systems are being considered as a suitable solution. However, WDM optical modules are too expensive for use in those areas, because the cost of accurately mounting and packaging the optical components is relatively high. Development of an inexpensive optical waveguide chip to reduce the mounting cost has been required for a long time.⁽¹⁾ On the other hand, the mounting of optical devices to an optical wiring board has also been studied widely in recent years. Here, small size and a high-density optical interconnection technology between surface mount devices are also required.⁽²⁾

Light-induced optical waveguides⁽³⁾ and self-written optical waveguides⁽⁴⁻⁶⁾ were developed in the early 1990s by creating optical waveguides in photopolymerizing resin using the self-trapping effect. However, since the cladding of these optical waveguides is a liquid resin and the waveguide length is limited to several millimeters at most, it was thought that practical utilization of this was going to be difficult. In 2001, for the first time, we realized the growth of straight optical waveguides with a uniform diameter which were more than 20 mm in length.⁽⁷⁾ In that paper, we demonstrated that all-solid polymer 3-D waveguide devices can be formed from a resin mixture solution. In the growth of these devices the core was formed by the selective polymerization of a high refractive index monomer, while the simultaneous hardening of both constituent monomers forms the cladding. We called this type of waveguide a Light-Induced Self-Written (LISW) optical waveguide. LISW technology forms an optical path by self-organization, and is expected as only assemble technology which corrects an optical off-axis resulting in module fabrication process. Furthermore, this technology enabled the realization of automatic optical fiber connections and packaging processes without the need for any dicing or polishing processes. Following this, some modified methods for LISW were

Reprinted from IEICE Trans. Electron. (<http://search.ieice.org/bin/index.php?category=C&lang=E&curr=1>), Vol.E90-C, No.5, pp.1061-1070, © 2007 IEICE, with permission from the IEICE (Permission No.10RB0078).

developed. Recently, many organizations have been studying the applications of this technology.⁽⁸⁻¹⁰⁾

In this invited paper, we will introduce various types of LISW optical technology from the basic concepts to their practical applications, mainly developed in our research group.

2. Principles

Self-focusing or the self-trapping phenomena of high-intensity light beams have been observed in various materials. This phenomenon has also been called a “spatial soliton”.⁽¹¹⁾ Many of these derive from material nonlinearities and the index change can be up to $\sim 10^{-3}$. Optical waveguides that form when an optical beam is self-trapped inside a nonlinear medium are of a transient nature, in the sense that they disappear when the input beam propagating as a spatial soliton is turned off. Photosensitive materials are the only ones in which the waveguide persists even after the beam is turned off. A permanent increase in refractive index of more than 0.02 can be attained in the light-induced waveguide. In this section, we introduce LISW optical waveguide technology using a photopolymerizing resin.

2.1 Growth mechanism

The principles of the formation of a LISW optical waveguide are shown in **Fig. 1**. First, the tip of an optical fiber is soaked in a photopolymerizing resin. Gaussian-like radiation from the fiber expands into the resin (**Fig. 1(a)**). The resin begins curing from the core tip, where the light is most intense (**Fig. 1(b)**) and the core starts to grow longitudinally due to the self-

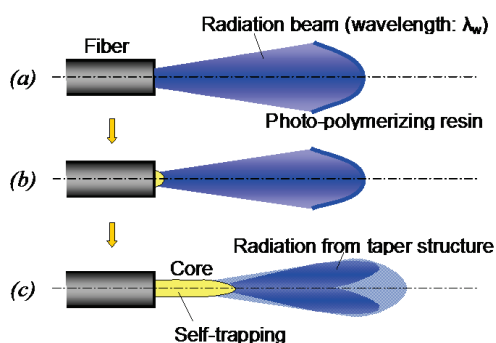


Fig. 1 LISW waveguide growing mechanism.

trapping mechanism of the radiated beam in the cured core (**Fig. 1(c)**). Accordingly, rapid growth proceeds ahead of the core tip until the radiative power is attenuated. In the meantime, in the weak radiation region at the sides of the core, the growth proceeds gradually until the radiation has abated due to internal reflection at the core/cladding boundary. As a result, a straight, uniform-diameter waveguide is produced. Though the photo-initiator used is sensitive at the writing wavelength λ_w , there is almost no absorption at the actual communication wavelength, which is much longer than λ_w .

2.2 Waveguide shape control⁽¹²⁾

First, we investigated the core formation characteristics. **Figure 2** shows a scanning electron microscope image of a typical cured core. Generally, the straight part of the core consists of two continuous sections. At the beginning of the core formation is a taper section, which is fixed to and starts from the center of the fiber. As the core is created, this expands axisymmetrically with respect to the fiber-axis (**Fig. 2(a)**). After this, a straight waveguide with uniform diameter is continuously created with a length of more than 30 mm (**Fig. 2(b)**). The surface of the core is very smooth (**Fig. 2(c)**). In the initial stage, the taper is induced by leakage from the radiation beam until the entire propagation mode is completely confined within the core. In addition, this tapered part gives rise to a highly directional beam, which converts the higher propagation modes to a lower propagating angled ray. As a result, a uniform diameter is maintained as curing

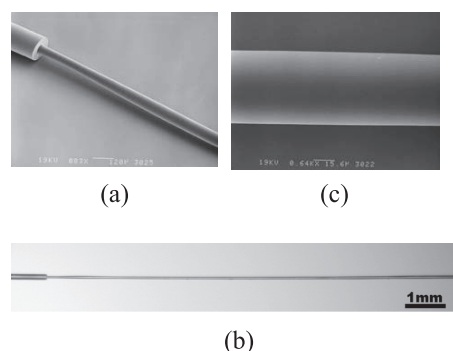


Fig. 2 Some images of LISW optical waveguides after the un-polymerised resin was removed by a solvent, (a) SEM image of initial part fixed to the GI100/140 fiber tip, (b) microscope photo of the LISW optical waveguide, (c) SEM image of the straight part after 10 mm of growth.

continues and the waveguide grows.

The tapered shape is strongly affected by the modal distribution in the optical excitation beam, represented by the far field pattern (FFP) and the near field pattern (NFP). We characterise the LISW optical waveguide by the diameter at the beginning and end of the taper part, D_a and D_b , respectively. To clarify the self-trapping action, we examined the taper section formation as follows. First, we plotted the initial diameter D_a versus the full width at $1/e^2$ maximum (FWEM) of NFP, as shown in Fig. 3(a). Because the light intensity at this position in fact corresponds to NFP, the initial diameter D_a changes linearly with the FWEM of NFP. This result shows D_a could be well defined by using NFP only. We also plotted the diameter at the taper end D_b , and the average taper angle α versus the full angle at $1/e^2$ maximum (FAEM) of FFP, as shown in Fig. 3(b) and Fig. 3(c), respectively. These plots show an almost direct relationship. These results suggest that the taper part is automatically formed until the entire propagating

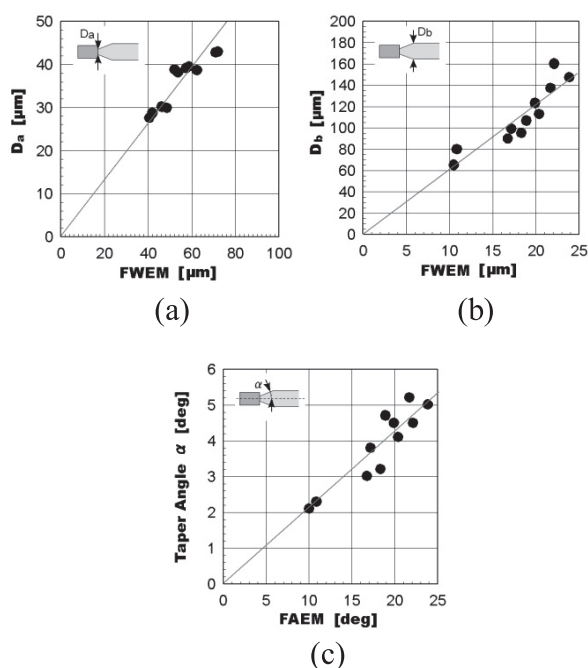


Fig. 3 The relationships between the waveguide shape and the characteristics of the irradiation beam from the GI100/140 (NA0.28) optical fiber. The samples of waveguide were prepared using acrylic photopolymerizing resin with $\lambda_w = 488 \text{ nm}$, $P = 380 \text{ mW}$ and $t = 50 \text{ sec}$ irradiation. (a) Initial diameter D_a versus FWEM estimated from NFP measurements, (b) waveguide diameter D_b versus FAEM estimated from FFP measurement, (c) taper angle α versus FAEM estimated from FFP measurement.

mode is confined by the refractive index difference between the cured resin and the uncured liquid resin, irrespective of the NA of the optical fiber that is being used. Furthermore, waveguide shape control can be realized by arbitrary launch conditions to the fiber, such as input NA and input position.

2.3 “Optical solder” effect by LISW

LISW waveguides are an attractive and practical process for realizing alignment between an optical fiber and a waveguide compared with other alignment systems such as the Si V-groove technique or active alignment. Because the waveguide structure is produced automatically from the fiber tip and has a circular cross-sectional shape (the same as the fiber), no misalignment occurs between the optical fiber and the waveguide. Although the starting position of the waveguide is accurate, the terminal position, which corresponds to the module end-face (see Fig.16), causes scattering due to heat convection reactions, gravity, and so on. To resolve this, we can utilize a LISW-specific effect which we call the “optical solder” effect.^(5,13,14) The “optical solder” effect makes it possible to realize a waveguide connection between two faceted fibers, even if a significant gap and a small degree of misalignment exist. The LISW waveguides grow towards each other from both sides to a central point where the opposing beams overlap and are then combined into one waveguide, as shown in Fig. 4.

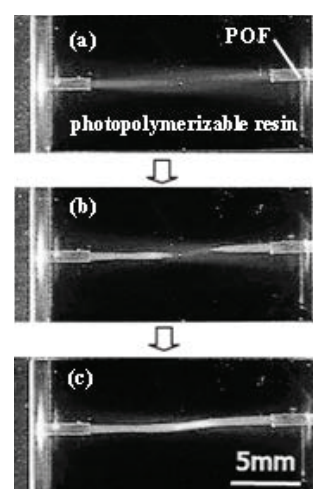


Fig. 4 The growth process of a bi-directional irradiation LISW optical waveguide using two $700 \mu\text{m}$ -diameter plastic optical fibers. (a) Initial stage of irradiation, (b) growth process, (c) terminal stage of irradiation.

Moreover, this effect can be applied not only to thick multimode optical fibers but to fine singlemode optical fibers. **Figure 5** shows a photograph of the actual LISW waveguide core fabricated between the two singlemode fibers. The fibers were first set on a grooved substrate for approximate alignment. The distance between the fibers was about 150–300 μm . Then, a photopolymerizing resin for the core selective polymerization method (see Sect. 4.2) was used to fill in the whole area around the tips of both fibers.⁽¹⁵⁾ A similar process to that described above was performed by launching an Ar^+ laser beam into both fibers. The core grew simultaneously from both ends and became connected at around the mid-point between the fiber tips. From the figure, neither misalignment nor any change in the core size was observed, suggesting that the singlemode condition was maintained in the LISW waveguide region by the subsequent solidification of the cladding.

An insertion loss of 0.5 dB was measured by launching light at 1310 nm into the waveguide through one of the fibers and detecting the output power from the end of the other fiber. We have also performed the same experiment in a situation where there was a slight angle between the axes of the two fibers, and a smoothly bent waveguide core connected near the center without any misalignment was successfully fabricated. This indicates that a simple self-aligned connection can be obtained by using the LISW technique, even with off-axis conditions.

3. Three dimensional optical circuits

Because the LISW waveguide forms along the direction of the light path, 3-D optical waveguide

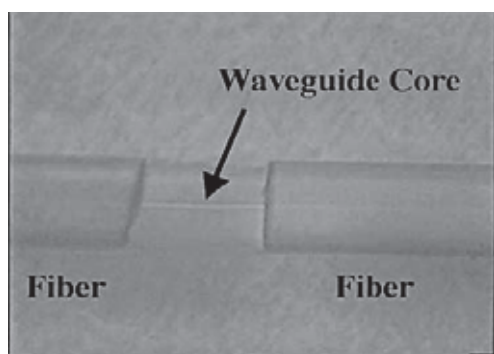


Fig. 5 Photograph of an optical interconnection using two single-mode fibers. A LISW waveguide was grown between the fibers.

components, such as branching or bending waveguides, can automatically be obtained if a half-mirror (at λ_w) or a mirror is inserted into the light path. In this section, we summarize the utilization of LISW technology for 3-D waveguide circuit formation and the improvements made in positional accuracy.

3.1 Transparent waveguides

Figure 6 shows an actual fabricated LISW waveguide grown toward a high transmission filter, (150 μm -thick borosilicate glass with $n_D = 1.522$), at an angle of incidence of 45° .⁽⁷⁾ The photograph was taken after withdrawing the core from the liquid cladding and subsequent removal of the uncured resin using acetone. Though the waveguide diameter slightly increases after passing through the filter, we once again observe the growth of straight waveguides from the back surface, in spite of the number of filters that have been inserted, as shown in the SEM photograph in Fig. 6(a). Figure 6(b) shows an enlarged photograph of a waveguide passing through the filter. In this picture a slight shift of the LISW waveguide's central axis is observed due to the refractive index difference between the filter and the optical waveguide. Because the waveguide is formed automatically along the light path, the loss due to misalignment should be very small, as long as the material chromatic dispersion is

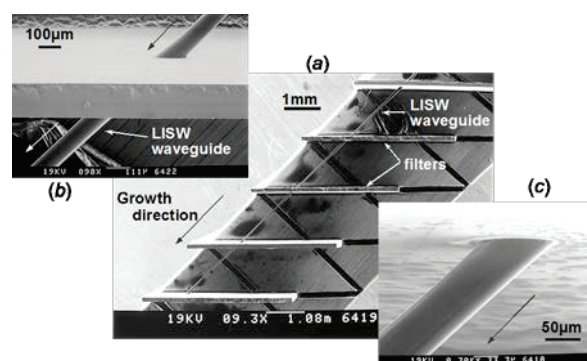


Fig. 6 Continuous LISW optical waveguide formed before and after a series of transparent filters at an angle of incidence of 45° . (a) LISW optical waveguide penetrating four transparent glass filters of 150 μm thickness. (b) Enlarged photograph showing the waveguide passing through one filter. The optical axis shift caused by the refraction can be observed. (c) Enlarged photograph of the point at which growth restarts at the back surface of the filter.

not extremely large. This loss can be negligible in common passive materials. Figure 6(c) is an enlarged photograph of the point from which the growth restarts from the back surface of the filter, and it demonstrates the excellent adhesion, linearity, and smoothness that can be obtained.

3.2 Reflecting waveguides

Figure 7 shows an optical microscope photograph of a LISW waveguide grown after reflection at a metal coated glass plate. Regardless of the metal layer being on the front or back surface of the glass plate, well defined LISW optical waveguides were obtained.⁽¹⁶⁾ With reflection at the front (Fig. 7(a)), the diameter of the waveguide is essentially maintained. The slight increase in core diameter is considered to be the result of increased light intensity at the bend. With reflection at the back (Fig. 7(b)), the waveguide becomes a little thicker due to the long free-space propagation in the glass. By employing this particular feature of LISW waveguides, we proved that a 90° optical path converter can be simply realized.

3.3 Accurate positioning

Mounting of an optical waveguide to an optical module requires very accurate positioning. In the case of LISW technology, because the waveguide structure is produced automatically from the fiber tip and has a circular cross-sectional shape (the same as the fiber), no misalignment occurs between the optical fiber and the waveguide. Although the starting position of the waveguide is accurate, the terminal position, which corresponds to the module end-face, causes scattering.

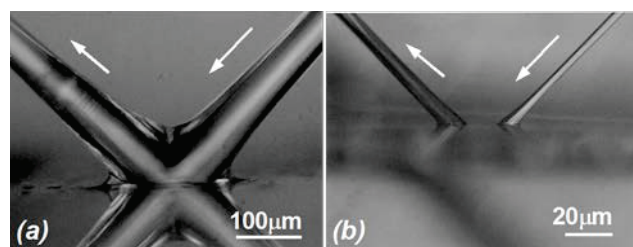


Fig. 7 Optical microscope photographs of 90° bends in waveguides fabricated with the use of a mirror. (a) Reflection at the substrate surface. (b) Reflection at the back surface of a 150- μm thick transparent glass sheet.

To resolve this, we utilized the LISW-specific “optical solder” effect described in Sect. 2.3.

The positioning accuracy was evaluated by measuring the center position of the waveguide, as shown in Fig. 8(a). Figure 8(b) shows a distribution map of the waveguide terminal position. The squares represent the positions at which the waveguide terminates, 11 mm from the end of the fiber, when fabricated using the unidirectional irradiation process, while the circles represent the positions at which the waveguide terminates when fabricated using the bi-directional irradiation process. From the figure, the positional accuracy of the unidirectional process is shown to be uncertain, mostly due to tilting of the fiber-tip, reaction heat convection, gravity, and so on. By contrast, high positional accuracy is achieved by a combination of the bi-directional irradiation process and a simple socket for fixing the enclosure. The standard deviation of the position when using a POF with a 700 μm diameter core was estimated to be 9.7 μm .⁽¹⁴⁾ These results suggest that optical devices, such as LEDs, LDs, and PDs, passive mounting are possible.

4. Cladding formation

Various applied technologies were developed using different hardening methods for the cladding and formation methods for the refractive-index distribution. By applying a suitable method, LISW waveguides can be obtained using all types of optical

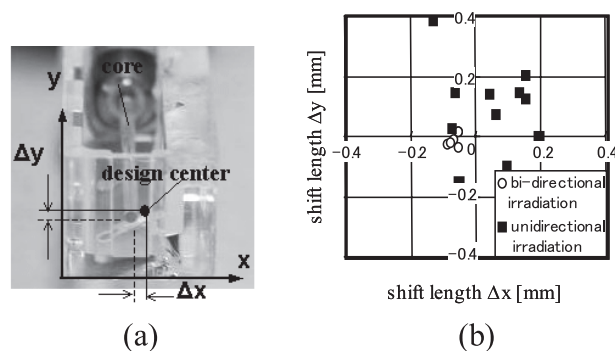


Fig. 8 Bi-directional waveguide formation, which grow the two waveguides toward the center position of the waveguide from the fiber and physical center of the module end-face until both waveguides joins together, to improve the positioning accuracy, (a) Method for measuring positioning accuracy, (b) Distribution map of waveguide terminal position employing a POF (Mitsubishi-Rayon, Eska-Miu).

fiber, e.g. a 9- μm diameter single mode silica fiber, GI50/125 & GI100/140 silica fiber, SI200/230 HCF fiber, GI120/230-POF, and SI980/1000-POF with 1 mm diameter. The LISW waveguide fabrication method can be classified into three main methods, the “Substitution method”, the “Core selective polymerization method”, and the “Cladding selective polymerization method”. These are summarized in **Table 1**. We can choose the optimal method from the table in consideration of the diameter and refractive index difference of the optical waveguide. In this section, we describe the process details and the performance obtained with each method.

4.1 Solution substitution method

With the “Solution substitution method”⁽¹⁷⁾ polymerization of the core and cladding layer is achieved using each pure solution individually. Because the solutions are introduced separately between the two polymerization processes, there is no mixing of the monomers involved, and a steep core/cladding boundary is obtained. However, since the waveguide is substantially damaged when the second solution is substituted for the first, this method is limited to optical fibers with a comparatively large diameter. **Figure 9** shows the process flow that we used to fabricate a WDM optical module, which we will discuss in Sect. 5.1. Firstly, a WDM filter is inserted into a slot angled at 45° in a miniature transparent plastic enclosure and an optical fiber is inserted into a socket in the enclosure (Fig. 9(a)). The enclosure is then filled with photo-

polymerizing resin with a higher refractive index, which will become the core of the waveguide (Fig. 9(b)). A laser at a wavelength of $\lambda_w = 405\text{--}488\text{ nm}$ is transmitted through the optical fiber to expose the resin. At the end of the fiber, the exposed resin starts to harden as described in Sect. 2.1, eventually forming the core of the waveguide. In this case, the WDM filter act as a half-mirror at λ_w , so the waveguide branches off (Fig. 9(c)). For example, the time required to form a 5-mm long branching waveguide is about 30 seconds. This time depend on the laser power and the reaction sensitivity of the material. Then the remaining un-hardened resin is removed using a solvent (Fig. 9(d)). Finally, the enclosure is filled with UV resin that has a lower refractive index (Fig. 9(e)). This forms the waveguide cladding, and the polymer module is completely hardened by UV illumination from all directions using a UV lamp (Fig. 9(f)).

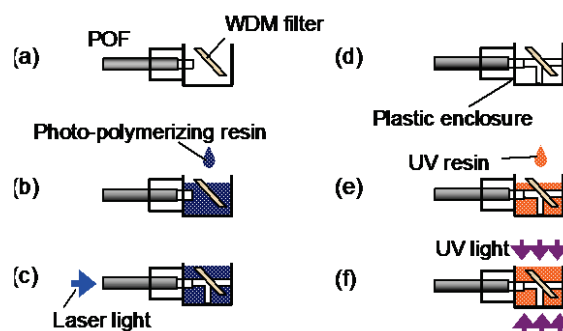


Fig. 9 Process flow used to fabricate a module.

Table 1 Various LISW technologies.

Method	Solution preparation & Mechanism	Monomer/oligomer status		Features		Ref.
		As core grown	As cladding cure	Typical properties	Refractive index profile	
Solution substitution	Core/cladding Substituti & simple polymerization	Core portion: Pure solid A Cladding portion: Liquid A	Core portion: Solid A Cladding portion: Solid B	Δn : no restriction Φ : $>200\mu\text{m}$ loss~0.2dB/cm (@650nm)		[7]
Core selective polymerization	Core/cladding Mixture & Selective polymerization with diffusion	Core portion: Solid A(rich)+liquid B Cladding portion: Liquid A+B	Core portion: Solid A(rich)+ B Cladding portion: Solid A+B	Δn : <0.03 Φ : $<200\mu\text{m}$ loss~0.4dB/cm (@650nm)		[7],[12] [15]
Cladding selective polymerization		Core portion: Solid B+liquid A Cladding portion: Liquid A+B	Core portion: Solid A+ B Cladding portion: Solid A+B(rich)	Δn : <0.02 Φ : no restriction loss~1dB/cm (@650nm)		[18]

A: higher refractive index oligomer, B: lower refractive index oligomer

The loss spectrum of a straight LISW waveguide fabricated using this process flow using a POF with a core diameter of 980 μm is measured by the cutback method, as shown in **Fig. 10**. The propagation losses at wavelengths of 650 nm and 525 nm are as little as 0.4 dB/cm and 0.5 dB/cm, respectively. Furthermore, the connection loss between the POF and the waveguide was very small, 0.1 dB. **Figure 11** shows the refractive index profile measured by an interference microscope. The interference fringes show that, the waveguide has a perfectly circular cross-section and a uniform index profile. The refractive index difference is estimated to be $\Delta n = 0.063$ ($NA = 0.45$), which is sufficiently larger than that of the POF ($NA = 0.25$). NA matching with the POF can easily be achieved by choosing a suitable cladding material.

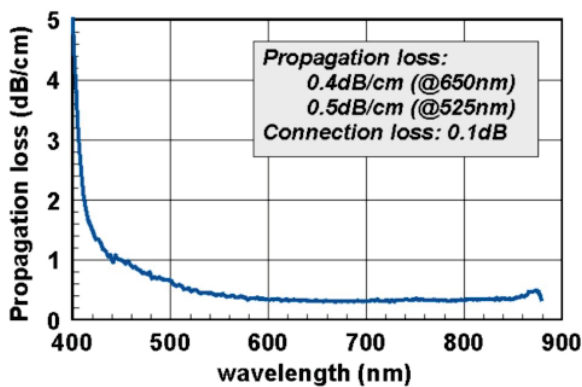


Fig. 10 Propagation loss spectrum of LISW waveguide fabricated by the solution substitution method.

4. 2 Core selective polymerization method

In order to avoid using the substitution process, which may cause damage to the optical waveguide, two kinds of selective polymerization methods were developed (**Fig. 12**). Both methods start by using a mixed solution consisting of two kinds of monomer for which the polymerization reaction mechanisms are different (Fig. 12(a)). In selective polymerization, a waveguide is formed by polymerizing one monomer selectively from the solution using the LISW technology (Fig. 12(b)). The “Core selective polymerization method” continuously polymerizes only photopolymer-A, which reacts with wavelength λ_w and has a higher refractive index than that of monomer B ($n_A > n_B$). Monomers A and B do not undergo copolymerization because the materials have different polymerization processes (Fig. 12(c)).

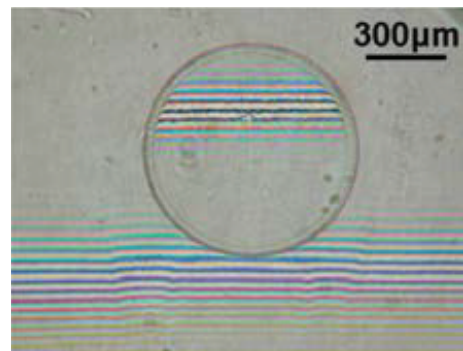


Fig. 11 Interference microscope photograph of core cross-section. A POF with 1 mm diameter is used to fabricate this waveguide.

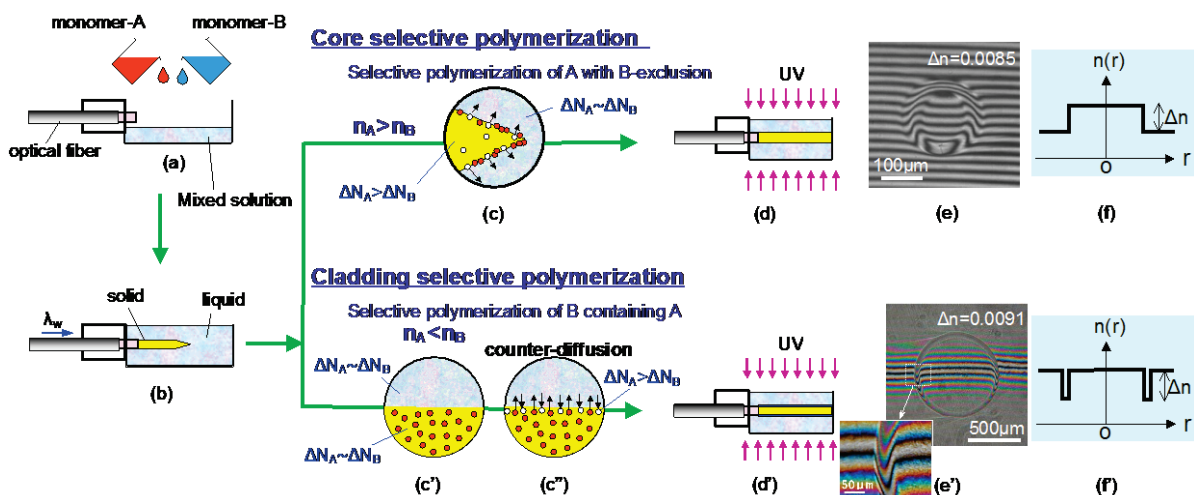


Fig. 12 Two kinds of selective polymerization LISW technologies.

Hardening of the cladding is carried out by exposing the whole of the mixed solution to ultraviolet light (Fig. 12(d)).

As an example, monomer A, which was used for the higher refractive index core, is a radical type resin made by blending acrylic acid and a urethane-acrylate oligomer. Monomer B, used for the lower refractive index material, is a cationic type fluorine inclusion epoxy. Monomer B has the following requirements: it must mix well and not co-polymerize with monomer A, it must not polymerize at the formation wavelength λ_w , and it must have a lower refractive index than that of monomer A. A photo-polymerizing resin containing a fluorinated epoxy monomer and a photo-initiator of 4,4'-Bis[di(β -hydroxy)phenylsulphonio]phenylsulfide-bis-hexafluoroantimonate satisfies these requirements. In the polymerization process (Fig. 12(c)), because only the photo-initiator for monomer A is sensitive to the wavelength being used, monomer A is polymerized selectively, and monomer B migrates through the mixture to the exterior of the core region. **Figure 13** shows the monomers actually used and the absorption spectra of the LISW optical waveguide obtained. The loss of the hardened waveguide is much larger than that of the two liquid monomers. After polymerization, scattering losses due to fluctuations in the degree of polymerization and phase separation of the two materials arise.

The core selective polymerization method can be applied to single-mode optical waveguide fabrication using a single-mode optical fiber.⁽¹⁵⁾ However, the main problem with this type of single-mode LISW

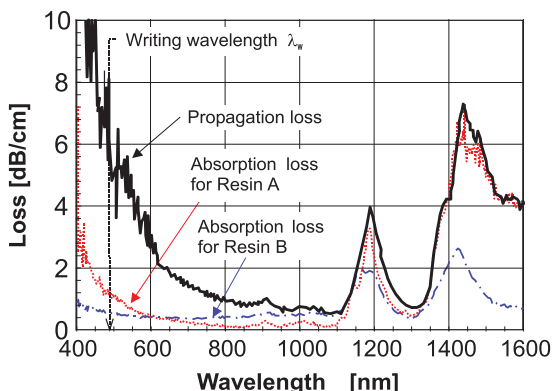


Fig. 13 Absorption spectra of the photo-polymerizing resins used, (before hardening), and propagation loss spectra of the LISW optical waveguide fabricated using a monomer mixture (A:B = 7:3) and a GI100/140 optical fiber (NA = 0.28).

waveguide is that the narrow waveguide core easily bends in the “liquid” resin mixture after the core is prepared by the process described above. In order to solve this problem, we tried performing UV exposure with the UV lamp in advance of the core formation process to increase the viscosity of the resin mixture. We call this partial hardening process the “pre-UV treatment.” **Figure 14** shows photographs of actual fabricated waveguide cores prior to the post-UV process: (a) without the pre-UV treatment and (b) after the pre-UV treatment was implemented. By comparing the two photographs it was confirmed that a straight LISW waveguide could be successfully realized by utilizing the pre-UV treatment in the process. Furthermore, the pre-UV treatment also furnished two other advantages: 1) the index difference between the core and the cladding was effectively reduced, leading to relaxation of the single-mode propagation condition, and 2) since less energy was required for the core formation, a longer waveguide was grown. The single-mode condition could be adjusted by choosing a suitable ratio for the mixture of the two monomers.

4.3 Cladding selective polymerization method

Finally, the “Cladding selective polymerization method”⁽¹⁸⁾ that enables the rapid growth of core is introduced. This technique utilizes the rapid polymerization of the low refractive-index Monomer B while incorporating a non-polymerizing Monomer A in the cured core with the same mixture ratio ($\Delta N_A \sim \Delta N_B$, Fig. 12(c')). A low refractive-index layer (cladding) is formed on the outside of the core as a result of the counter diffusion of monomers, and/or selective polymerization due to laser beam scattering

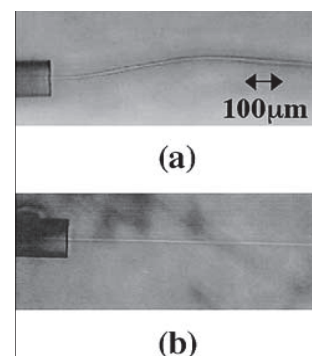


Fig. 14 Photographs of the waveguide core (a) without the pre-UV treatment and (b) with the pre-UV treatment.

(Fig. 12(c'')). In this method, only Monomer B polymerizes at λ_w . The low-refractive-index monomer of a cladding layer is consumed by polymerization, and, as a result, additional refilling of the low-refractive-index monomer is carried out by the counter diffusion from the mixture solution into this layer. In this cladding layer, the low refractive-index monomer content becomes greater than that of higher one ($\Delta N_A > \Delta N_B$). The refractive-index distributions of the waveguide sections produced by both selective polymerization methods are also shown in the Table 1. Some profile deformation around the boundary may be observed depending on the fabrication conditions (Fig. 12(e')).

We used a photopolymerizing resin mixture consisting of radical and cationic polymerizing monomers in order to satisfy the requirements of this method. Ethoxylated trimethylolpropane triacrylate (EO-TMPTA, average molecular weight $M_n = 428$, purchased from Sartomer, Co., Ltd.) was used for Monomer A. This is a radical polymerizing monomer with a lower refractive index, $n_A = 1.469$. Diglycidyl ester of bisphenol A (DGEBA, $M_n = 398$, purchased from Dow Chemical Company) was used for Monomer B. This is a cationic polymerizing monomer with a higher refractive index, $n_B = 1.569$. The ratio of the mixture, A:B was 6:4 in terms of weight. Photosensitive polymerization initiators were added to the monomer mixture to provide the correct conditions for the photochemical absorbance to be $\lambda_w < 490$ nm and $\lambda_c < 380$ nm. The photopolymerizing resin mixture showed excellent solubility and no cloudiness was observed. Its refractive index was $n_C = 1.509$ before photopolymerization and $n_C = 1.536$ after UV curing.

In addition, IR spectroscopy was used for chemical analysis of the composition distribution over the core-cladding region. Using the peak positions of the IR absorbance spectra at 1511 cm^{-1} and 1739 cm^{-1} , which originate from the C = O structure of EO-TMPTA and the benzene nucleus of DGEBA respectively, we can estimate their distribution, as shown in Fig. 15. This curve agrees with the actual refractive index distribution. From the chemical analysis, these results imply that the enrichment of monomer A due to the counter diffusion phenomenon is about 10%.

5. Optical module

POFs have been considered to have potential uses in both automotive and home network applications.

Using the LISW technique, we have successfully fabricated and tested a POF WDM optical module containing 3-D optical circuits and a specially designed WDM filter. Here, we describe its optical properties.

5.1 POF-visible WDM module

As one of the potential applications, we proposed a WDM communication module using a POF and LEDs (which are excellent in terms of heat stability and system costs). To reduce both process and assembly costs dramatically, we investigated a unique WDM module fabrication technique using polymer materials.

For the simplest configuration, we proposed a bi-directional communication module using a single POF and two LEDs (different wavelengths).⁽¹⁷⁾ This system is promising compared to existing fiber networks because it reduces the quantity of fiber needed by half, its flexibility is greater (which makes it easier to install) and the space taken up by the connections is reduced. This type of module can be applied to a number of topologies, such as tree, active-star and ring topologies. To realize an optically complex bi-directional module with a simple fabrication process, we employed the solution substitution method of the LISW technique.

Figure. 16 shows a schematic diagram of a pair of LISW optical waveguide modules that are connected using an in-line POF connector for bi-directional single POF communication. The modules include a three-

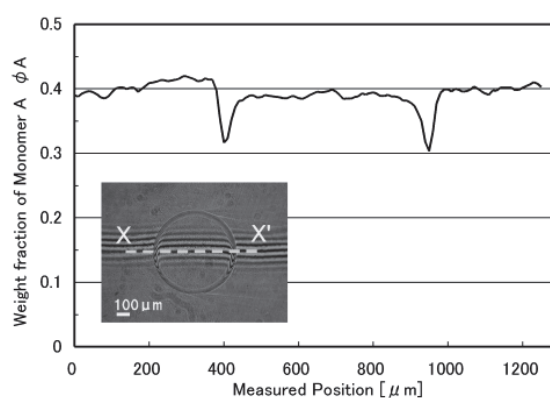


Fig. 15 Calculated composition over cross-section (X-X') of the waveguide from IR spectroscopy analysis. LISW optical waveguides were prepared with an irradiation power of 5mW ($\lambda_w = 458$ nm), irradiation time of 15 sec and counter diffusion time of 60 min and cut at a length of 1 mm from the end face of the fiber for this measurement.

dimensional optical circuit, consisting of a WDM filter angled at 45° and a branching LISW waveguide, all contained in a miniature transparent plastic enclosure with a pig-tailed POF. The WDM filter has characteristics that enable transmission of green LED light and reflection of red LED light. The dimensions of the enclosure are 6 mm in width by 8 mm in length by 14 mm in thickness. Both ends of the branching LISW waveguide in the modules are used for the optical I/O ports, on which a green LED, a red LED and two PDs (photo diodes) are mounted. **Figure 17** shows an example of a completed module. It is evident from the figure that a branching LISW waveguide has certainly been formed. The insertion loss of the module is 2.1 dB for the green LED (495 nm) and 2.2 dB for the red LED (650 nm). These values include 1.3 dB of structural loss of the T-junction waveguide and filter loss through the high NA modules.

A dielectric multilayer type WDM filter was designed for use with a multimode waveguide to

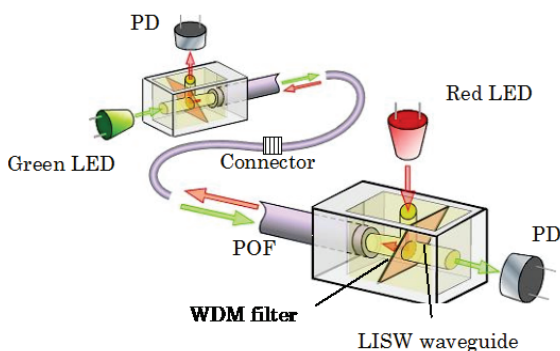


Fig. 16 Diagram of bi-directional single POF communication using the LISW optical waveguide modules.

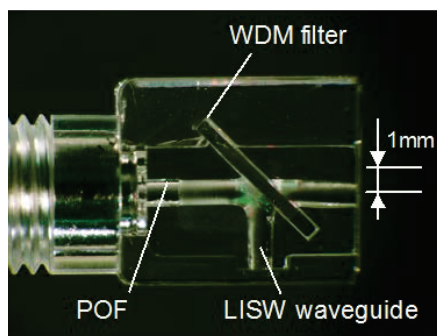


Fig. 17 Example of a completed LISW waveguide module fabricated by using the solution substitution method. The photo is taken before pouring the cladding material.

obtain high performance. In general, when a WDM filter is used with a multimode waveguide, higher order rays must be considered because these rays may result in excess optical losses in the filter. Accordingly, the filter was designed to achieve low optical losses from both low and high order rays that could propagate in the POF.

A green LED, a red LED and two pin-PDs that could respond at over 250 Mbit/s were mounted on each of the optical ports of the modules using an active alignment process. At this time, additional WDM filters were inserted in front of the PDs in order to avoid optical crosstalk from local LEDs. In future, these additional filters will be removed when the problem of optical crosstalk has been overcome. The coupled power of the LEDs into the waveguides was -5.7 dBm for the green LED and -1.5 dBm for the red LED for modulated light signals.

5. 2 BER (bit error rate) measurement

The BER was measured in both half-duplex and full-duplex modes. **Figure 18** shows that the power penalty due to crosstalk, taken from a comparison of half-duplex (H.D.) and full-duplex (F.D.) modes, was about 0.2 dB for the red and green modules. The PD input power in full-duplex mode at a BER of 10^{-12} was -17.4 dBm for the green LED and -20.6 dBm for the red LED. The difference in these results is attributed to the sensitivity of the PDs and the quality of the waveforms of the LEDs. These results and the coupled optical powers of the LEDs (described previously) determined that the power budget of this system would be 11.7 dB

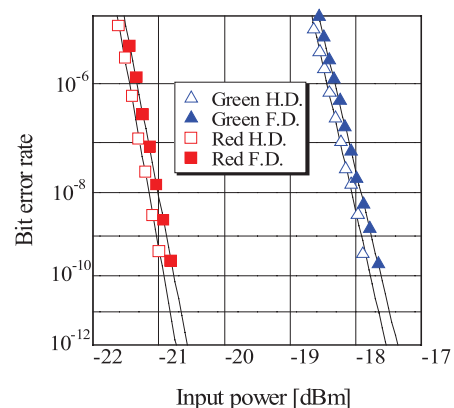


Fig. 18 Results of the BER measurements at a data rate of 250 Mbps, and PRBS 27-1, NRZ signal. H.D. and F.D. denote the half-duplex and full-duplex communication modes, respectively.

for the green LED and 19.1dB for the red LED. Thus, the maximum transmission length of this system was limited by the green LED. If a POF was to be connected between the pair of optical transceivers with two inline connectors, the maximum feasible length of the POF is estimated to be more than 20 m from the power budget and the individual insertion losses of the two modules ($2.1 \text{ dB} \times 2$), the two inline connectors ($0.8 \text{ dB} \times 2$) and the transmission loss of the POF (0.14 dB/m) with a 3 dB power margin. This length is considered to be sufficient to cover most home and automotive applications. These results convey the excellent properties of LISW optical waveguides and highlight the potential of the LISW technique for low cost fabrication and packaging.

6. Conclusion

In this paper, we summarized the principle and applications of Light-Induced Self-Written (LISW) optical waveguide technologies mainly developed by our research group. LISW technology has many possible applications not only toward low-cost optical interconnection but also expansion to the creation of various potential devices. Of the applications of this technology, those being most actively pursued are three-dimensional high-density parallel connections in an optically integrated circuit and optical wiring in an electronic mixed-loading substrate. However, application studies have only just begun and some areas still remain unexplored before full-scale utilization is possible. Especially, LISW technology is expected to be important in applications in the field of consumer electronics, for which the demand for low cost is strong. In order to realize actual devices, which can meet existing and future required standards, it will first be necessary to develop highly reliable and high productivity materials, and to optimize the structures.

Acknowledgments

The authors are pleased to acknowledge Prof. Kaino and Associate Prof. Sugihara of Tohoku Univ., Prof. Okamoto and Dr. Tomiki of Shizuoka Univ., and Mr. Inui of Toyoda Gosei Co. Ltd. for many fruitful discussions.

References

- (1) Mizuno, H., Sugihara, O., Jordan, S., Okamoto, N., Ohama, M. and Kaino, T., "Replicated Polymeric Optical Waveguide Devices with Large Core Connectable to Plastic Optical Fiber using Thermo-plastic and Thermo-curable Resins", *J. Lightwave Technol.*, Vol.24, No.2 (2006), pp.919-926.
- (2) Choi, C.-G., Han, S.-P. and Jeong, M.-Y., "Two-dimensional Polymeric Optical Waveguides for High-density Parallel Optical Interconnection", *Opt. Comm.*, No.235 (2004), pp.69-73.
- (3) Frisken, S. J., "Light-induced Optical Waveguide Uptapers", *Opt. Lett.*, Vol.18, No.13 (1993), pp.1035-1037.
- (4) Kewitsch, A. S. and Yariv, A., "Self-focusing and Self-trapping of Optical Beams upon Photopolymerization", *Opt. Lett.*, Vol.21, No.1 (1996), pp.24-26.
- (5) Hatakeyama, I., Ichige, K. and Yamaguchi, K., "An Observation of the Connecting Path of the Phase Conjugate Wave Propagated through Two Different Kinds of Fibers", *IEICE Trans. Electron.* (Japanese Edition), Vol.J81-C-I, No.9 (1998), pp.560-561.
- (6) Shoji, S. and Kawata, S., "Optically Induced Self-growing of Fiber Structure in a Photopolymerizable Resin", *Proc. SPIE*, Vol.3740 (1999), pp.376-379.
- (7) Kagami, M., Yamashita, T. and Ito, H., "Light-induced Self-written Three-dimensional Optical Waveguide", *Appl. Phys. Lett.*, Vol.79, No.8 (2001), pp.1079-1081.
- (8) Dorkenoo, K., Crécut, O., Mager, L., Gillot, F., Carre, C. and Fort, A., "Quasi-solitonic Behavior of Self-written Waveguides Created by Photopolymerization", *Opt. Lett.*, Vol.27, No.20 (2002), pp.1782-1784.
- (9) Yamashita, K., Hashimoto, T., Oe, K., Mune, K., Naitou, R. and Mochizuki, A., "Self-written Waveguide Structure in Photosensitive Polyimide Resin Fabricated by Exposure and Thermosetting Process", *IEEE Photonics Technol. Lett.*, Vol.16, No.3 (2004), pp.801-803.
- (10) Ozawa, H., Obata, Y., Mimura, Y., Mikami, O. and Shioda, T., "Self-written Waveguide Connection Across Diced Waveguide Gaps", *IEEE Photonics Technol. Lett.*, Vol.18, No.7 (2006), pp.880-882.
- (11) Kivshar, Y. S. and Agrawal, G. P., *Optical Solitons* (2003), Academic Press.
- (12) Yamashita, T., Kagami, M. and Ito, H., "Waveguide Shape Control and Loss Properties of Light-induced Self-written (LISW) Optical Waveguides", *J. Lightwave Technol.*, Vol.20, No.8 (2002), pp.1556-1562.
- (13) Yoshimura, T., Inoguchi, T., Yamamoto, T., Moriya, S., Teramoto, Y., Arai, Y., Namiki, T. and Asama, K., "Self-organized Lightwave Network Based on Waveguide Films for Three-dimensional Optical Wiring within Boxes", *J. of Lightwave Technol.*,

Vol. 22, No.9 (2004), pp.2091-2100.

- (14) Matsui, T., Yamashita, T. and Kagami, M.,
 “Improvement in Positioning Accuracy of Light-
 induced Self-written Polymeric Optical
 Waveguide using an “Optical Solder” Effect”,
Japan. J. Appl. Physics, Vol.45, No.38 (2006),
 pp.L1033-L1035.
- (15) Sugihara, O., Tsuchie, H., Endo, H., Okamoto, N.,
 Yamashita, T., Kagami, M. and Kaino, T., “Light-
 induced Self-written Polymeric Optical Waveguides
 for Single-mode Propagation and for Optical
 Interconnections”, *IEEE Photon. Technol. Lett.*,
 Vol. 16, No.3 (2004), pp.804-806.
- (16) Kagami, M., Yamashita, T. and Kawasaki, A.,
 “Three-dimensional Optical Waveguide Circuits
 using a Light-induced Self-written Technology”,
R&D Review of Toyota CRDL, Vol.37, No.1 (2002),
 pp.43-50 (in Japanese).
- (17) Yonemura, M., Kasawaki, A., Kato, S., Kagami, M.
 and Inui, Y., “Polymer Waveguide Module for Visible
 Wavelength Division Multiplexing Plastic Optical
 Fiber Communication”, *Opt. Lett.*, Vol.30, No.17
 (2005), pp.2206-2208.
- (18) Yamashita, T. and Kagami, M., “Fabrication of Light-
 induced Self-written Waveguides with a W-shaped
 Refractive Index Profile”, *J. of Lightwave Technol.*,
 Vol.23, No.8 (2005), pp.2542-2548.

Manabu Kagami

Research Fields :

- Optical communication devices
- Optical sensor

Academic Degree : Dr. Eng.

Academic Societies :

- IEICE
- The Japan Society of Applied Physics
- The Optical Society of Japan
- The Society of Automotive Engineers of Japan
- The Japan Institute of Electronics Packaging
- IEEE
- The Optical Society of America

Awards :

- Best Paper Award of IEICE, 2008
- Best Paper Award of IEEE CPMT Symposium
Japan, 2010



Tatsuya Yamashita

Research Fields :

- Photonic integrated circuits
- Optical communication systems

Academic degree : Dr. Eng.

Academic Societies :

- IEICE
- The Japan Society of Applied Physics
- The Optical Society of Japan
- The Optical Society of America

Awards :

- Young Scientist Award for the Presentation of
an Excellent Paper on the 11th JSAP, 2001
- Best Paper Award of IEICE, 2008
- Best Paper Award of IEEE CPMT Symposium
Japan, 2010



Masatoshi Yonemura

Research Fields :

- Optical communication devices
- Optical sensor

Academic Society :

- IEICE

Award :

- Best Paper Award of IEICE, 2008



Takayuki Matsui

Research Fields :

- Optical devices
- Plasmonics

Academic Societies :

- IEICE
- The Japan Society of Applied Physics

Award :

- Best Paper Award of IEICE, 2008

